Journal of Materials Chemistry A

Accepted Manuscript

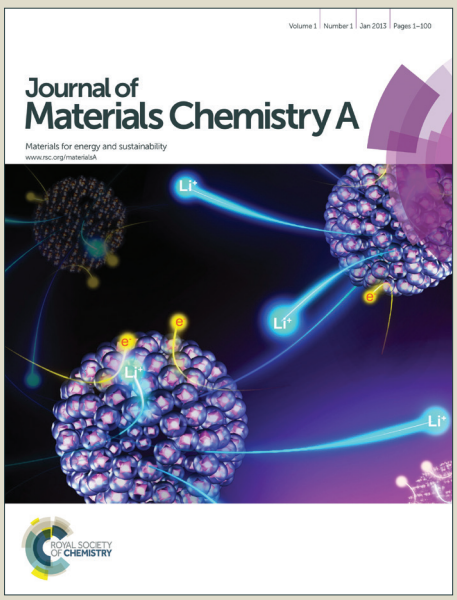

ROYAL SOCIETY OF CHEMISTRY

www.rsc.org/materialsA

Journal of Materials Chemistry A

Journal of Materials Chemistry A

Dynamic Article Links►

Cite this: DOI: 10.1039/c0xx00000x

ARTICLE TYPE

www.rsc.org/xxxxxx

Metal-organic frameworks with inherent recognition sites for selective phosphate sensing through their coordination-induced fluorescence enhancement effect

Jian Yang, Yan Dai, Xiangyang Zhu, Zhe Wang, Yongsheng Li, Qixin Zhuang, Jianlin Shi, and Jinlou Gu*

Received (in XXX, XXX) XthXXXXXXXXX 20XX, Accepted Xth XXXXXXXXX 20XX
DOI: 10.1039/b000000x

Luminescent metal-organic frameworks (LMOFs) have attracted great attention as a unique class of sensing materials. In this work, the intrinsically fluorescent amino derivative of UiO-66 (UiO-66-NH_2) was successfully exploited as a fluorescent probe for the sensitive and selective phosphate anion detection in aqueous medium. The inorganic Zr-O clusters and organic BDC-NH_2 linkers in the elaborated UiO-66-NH_2 MOFs were individually designed as phosphate recognition sites and signal reporters. The intrinsic fluorescence of BDC-NH_2 was tuned from high to weak emission by ligand-to-metal charge transfer (LMCT) upon its integration into the framework of UiO-66-NH_2 MOFs, and this weakened fluorescence could be proportionally recovered in correlation with the applied phosphate level through a newly developed competitive coordination effect. The specificity to phosphate recognition of the employed sensory platform was scarcely affected by other possible interfering species. The efficacy of this strategy was demonstrated by a linear phosphate detection range of 5-150 μM and detection limit of 1.25 μM, which was far below the detection requirement of phosphate discharge criteria in the water environment. The possible sensing mechanisms for anionic phosphate detection using the currently established fluorescent probe, including host-guest interaction and structure-property correlation, were systematically investigated by XPS, FT-IR, XRD, TEM and N_2 sorption techniques.

Introduction

Phosphate plays a critical role in biological system, and the determination of its concentration in body fluids is helpful for the diagnosis of several diseases such as hyperparathyroidism and fanconisyndrome.[1,2] Meanwhile, it is generally the limiting nutrient in water environment, which is responsible for severe environment issues such as eutrophication.[3] Therefore, a reliable, sensitive and selective method for the detection of phosphate in water is of great significance for the human health and environment protection.

Among various strategies for the quantitative detection of phosphate,[4-6] fluorescent technique has attracted wide attention due to their exquisite advantages such as high sensitivity, simple operation, and superb spatial and temporal resolutions.[7,8] However, it is generally a challenge for selective and reliable sensing of anions in aqueous medium due to their strong hydration effect, which requires strong affinity between recognition sites and analytes.[9] Meanwhile, traditional molecular fluorescent probes are usually applied in homogenous assay systems, which meets some difficulties in the separation for the recycling and poor water solubility for the analysis in aqueous solution.[10] To enhance the efficacy of fluorescent sensing events, extensive efforts have been currently devoted to the design of heterogeneous system, such as to integrate molecular fluorescent probes in a support matrix, for the detection of anions.

Metal-organic frameworks (MOFs), composing of organic struts with inorganic nodes, feature high surface areas, versatile framework compositions and exposed active sites.[11-13] Thanks to these excellent characteristics, they have been regarded as one of the leading candidates for sensing materials.[14-17] Especially, luminescent MOFs (LMOFs) have been successfully exploited as a unique class of sensing platform with many obvious advantages.[18-21] Their intrinsic porosity and functional groups promote preferred analyte binding and pre-concentrate the guest molecules in the network, benefitting to the selective and sensitive detection. Additionally, the crystalline nature of LMOFs, compared with amorphous materials, makes it easy to identify and investigate the structure-property correlation.[22] Up to now, several LMOFs have been utilized as platforms for ions, small molecules and gas detections.[23-33] Notably, Lv and co-workers recently reported a QDs-MOFs system to assess the phosphate in environmental aqueous samples, which utilized the MOF-5 to quench the fluorescence of ZnO QDs by an electron-transfer process.[34] However, this reported sensor essentially recurred to

the luminescence in QDs and focused on the interaction between QDs and MOFs. In contrast, a simpler strategy utilizing the inherent fluorescence of MOFs as a sensory reporter, spontaneously integrating with the phosphate recognition sites seems more desirable while more challengeable.

Very recently, we found that Zr-based MOFs (ZrMOFs) presented high affinity towards phosphoric groups.[35,36] It was verified that the Zr-O nodes in MOFs served as specific anchorages for the effective capture of phosphor bearing phosphates or phosphonates *via* the formation of Zr-O-P bonds. This promotes us to further propose an idea that the ZrMOFs may also work as sensing platforms for the selective recognition and detection of inorganic phosphate in aqueous solution. Meanwhile, a consensus has been reached that the ZrMOFs possess exceptional chemical and thermal stability.[37,38] The crystalline structure could be maintained even there are a large number of missing-linker defects, which implies that the bonds between the Zr-O clusters and carboxylic groups in organic struts could be partially broken or reformed without structural collapse.[39] These merits of ZrMOFs, including stable architecture, exchangeable organic ligands and specific recognition function, meet the criteria in the design of phosphate sensor provides that sensitive fluorescent reporter is also integrated.[40] Therefore, the critical prerequisite is to find a reasonable fluorescent subunit, which could not only be easily modulated into the framework of MOFs as organic struts, but also could provide an obvious fluorescent signal for the transducer.

It is noticed that the simple molecule of 2-amino-1,4-benzenedicarboxylate (BDC-NH_2) is intrinsically luminescent. Since the amino group in 1,4-benzenedicarboxylate (BDC) is of electron-donating, it provides the lone pair of nitrogen for the interaction with the π*-orbital of the benzene ring, and consequently enhances the fluorescent efficiency of parent BDC.[41] Meanwhile, the amino derivative of UiO-66 (UiO-66-NH_2) could be facilely fabricated with a similar structure to its prototype ZrMOFs of UiO-66, except it utilizes BDC-NH_2 linkers instead of BDC.[42] These strongly motivate us to explore a simple and novel strategy, in which the Zr-O clusters and BDC-NH_2 ligands in the resultant UiO-66-NH_2 MOFs are designed as recognition sites and signal reporters for the phosphate assay, respectively (Scheme 1).

Scheme 1. Schematic illustration of phosphate coordination-induced fluorescence enhancement effect in MOFs of UiO-66-NH_2 for the selective and sensitive phosphate detection with inorganic nodes as natural recognition sites and organic struts as fluorescent reporter.

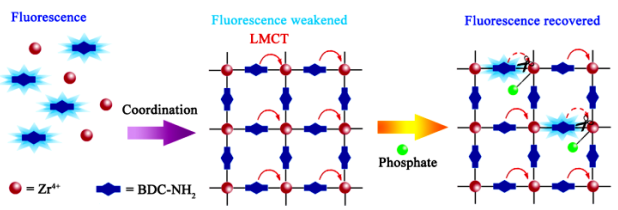

As expected, the fluorescence of free BDC-NH_2 could be tuned from high to weak emission, which was mainly ascribed to the ligand-to-metal charge transfer (LMCT) upon its coordination with Zr-O clusters to form the network of UiO-66-NH_2 MOFs.[41] On the other hand, the inorganic phosphate exhibits high affinity towards the Zr-O nodes in UiO-66-NH_2 so that it could be specifically recognized in aqueous solution.[35,36] Additionally, the phosphate demonstrates a competitive coordination effect with carboxylic groups in BDC-NH_2, which further weakens the interaction between inorganic Zr-O nodes and organic struts of BDC-NH_2. As a consequence, once the phosphate interacts with the framework of UiO-66-NH_2, the LMCT is subject to undermine. The original fluorescence of BDC-NH_2 ligands is proportionally recovered in correlation with the level of the applied phosphate. In the current work, the selective and sensitive detection of phosphate in aqueous solution with a linear range of 5-150 μM and detection limit of 1.25 μM has been achieved by this newly established strategy.

Experimental section

Chemicals and materials

Zirconyl chloride octahydrate ($ZrOCl_2$ $8H_2O$) and benzoic acid were purchased from Sinopharm Chemical Reagent Co., Ltd, China. KH_2PO_4, N,N-dimethylformamide (DMF), ethanol and HCl (37%) were obtained from Shanghai Lingfeng Chemistry Reagents Co., Ltd, China. BDC-NH_2 and HEPES (4-(2-hydroxyethyl) piperazine-1-ethanesulfonic acid) were supplied by Sigma-Aldrich. The solutions of various anions were prepared by dissolving Na_2SO_3, Na_2SO_4, Na_2CO_3, $NaHCO_3$, NaCl, $NaNO_3$, KBr (Sinopharm Chemical Reagent Co., Ltd) in aqueous solutions, respectively. All reagents were of analytical grade and used as received without additional purification.

Preparation of UiO-66-NH_2

UiO-66-NH_2 was prepared using the reported solvothermal method with slight modification.[42] Briefly, $ZrOCl_2$ $8H_2O$ (0.645 g, 2 mmol), BDC-NH_2 (0.362 g, 2 mmol), benzoic acid (4.885 g, 40 mmol) and concentrated HCl (0.347 mL) were mixed with DMF (34 mL) in a 100 mL Teflon-lined stainless steel autoclave, which were kept in an oven at 120 ^{o}C for 24 h. After cooling down to room temperature, the yellow powder was centrifuged and washed with DMF (3 × 20 mL) over a 12 h period to remove the unreacted ligands and metal ions. The DMF was then replaced with ethanol (3 × 20 mL) over a two-day period. Finally, the solid was dried at 80 ^{o}C *in vacuo* for 24 h to obtain the synthesized UiO-66-NH_2.

Phosphate anion sensing properties

The suspension of fluorescent probe was prepared by dispersing 50 mg of UiO-66-NH_2 nanoparticles in 1000 mL HEPES buffer solution (pH = 7, 20 mmol) under ultrasonic condition for 20 min. The probe suspension was preserved in a refrigerator at 4 ^{o}C under dark condition. Then, to study the response kinetics, the phosphate was added to the above fluorescent probe suspension to achieve the buffer solution with phosphate anion concentration of 100 μM, and the fluorescent intensity were recorded at different time with an excitation wavelength at 328 nm.

To explore the ability of UiO-66-NH_2 fluorescent probe for phosphate anion detection, 3 mL of UiO-66-NH_2 suspension and the different concentrations of (30 μL) phosphate anion solutions

were sequentially added to a quartz cuvette. After incubating for 90 min at 30 °C, their fluorescence spectra were recorded. To investigate the interference effects of the co-existent anions, the various anion solutions were added into the fluorescent probe suspension to achieve the co-existent anions concentration of 100 μM with or without phosphate anion (100 μM). The fluorescence measurements were conducted under otherwise the same conditions as the above phosphate anion sensing experiments.

Investigation of sensing mechanism

To probe the proposed phosphate coordination-induced fluorescence enhancement effect of the current fabricated chemosensors, the various properties of the resultant phosphate adsorbed UiO-66-NH_2 (UiO-66-NH_2(P)) (The molar ratio of Zr to P in solution was set as 1 : 0.6) were compared with those of the as-synthesized parent UiO-66-NH_2 through FT-IR, XPS, N_2 sorption and TEM techniques. Briefly, 50 mg of UiO-66-NH_2 powder was added to 20 mL of 10 mM phosphate solution (pH = 7, HEPES buffer). After incubating the mixture for 90 min at 30 °C, the suspension was centrifuged at 9000 rpm for 10 min and washed with deionized water for three times. Then, the powder was heated at 80 °C *in vacuo* for 24 h to obtain the UiO-66-NH_2 (P). The structure evolvement of UiO-66-NH_2(P) in correlation with the phosphate concentrations was traced by XRD measurement with different P : Zr molar ratio at ranges from 0 to 3 under otherwise the same condition as the above experiment.

Instruments and methods

Diffuse reflectance UV-Vis (DR-UV-Vis, UV-2550; Shimadzu, Japan) was employed to measure the optical absorption spectra. Fluorescence spectra were measured by spectro-fluorophotometer (RF-5301PC; Shimadzu, Japan). The powder XRD patterns were obtained on Bruker D8 using Cu Kα radiation (40 kV, 40 mA). N_2 sorption isotherms were recorded with surface area and pore size analyzer (Micromeritics Tristar 3020). All the samples were degassed under vacuum for 12 h before measurements. The specific surface area and micropore volume were calculated by the BET method using adsorption data at a relative pressure lower than 0.15. FT-IR was conducted on Nicolet 7000-C spectroscopy with a resolution of 4 cm^{-1} using the KBr method. XPS signals were collected on a VG Micro-MK II instrument. Transmission electron microscopy (TEM) was conducted on a JEM-2100F electron microscope. Thermogravimetric analysis (TGA) was conducted on a Perkin-Elmer thermogravimetric analyzer by heating the sample to 800 ℃ under air atmosphere (50 mL min^{-1}) at a heating rate of 10 ℃ min^{-1}.

Results and discussion

Characterization of UiO-66-NH_2

The powder XRD pattern of the synthesized UiO-66-NH_2 exhibits a typical *Fm*3*m* symmetric space group in consistent with the reported UiO-66 topology (**Fig. 1**).[37] The permanent porosity of the activated UiO-66-NH_2 is confirmed by the N_2 sorption isotherms at 77 K (**Fig. S1, ESI†**), which presents a type I isotherm with BET surface area and pore volume of 671 m^2/g and 0.67 cm^3/g, respectively. Another steep increase in the P/P_0 range of 0.85-1.0 should be ascribed to the interstices among the particles, indicative of the relative small particle size of the resultant MOFs.[43] These UiO-66-NH_2 nanoparticles with high permanent porosity could provide a natural space to accommodate the guest molecules, increasing the chances of guest-host interaction and benefitting to the sensitive detection of phosphate. TEM image (**Fig. S2A, ESI†**) further verifies that their particles size is in the range of 20-30 nm, which favours their dispersion in aqueous solution.

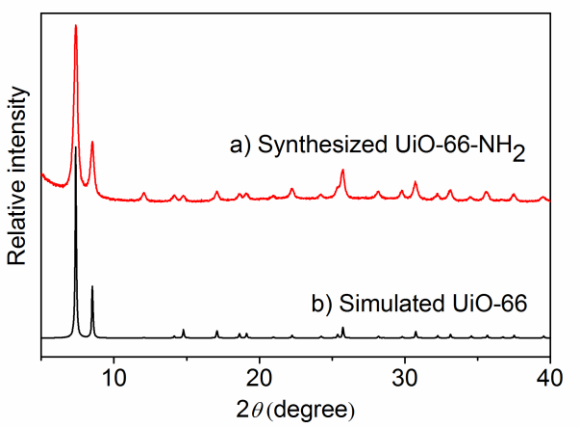

Fig. 1 Powder XRD patterns of (a) the as-synthesized UiO-66-NH_2 and (b) the simulated UiO-66.

The TGA data (**Fig. S3, ESI†**) reveal that UiO-66-NH_2 is stable up to 250 °C, and has a 43.3% weight loss (250-510 °C) corresponding to the decomposition of BDC-NH_2 linkers. From the weight loss and the preserving mass for zirconia, the number of BDC-NH_2 in each unit is calculated to be less than the theoretical unit composition of $Zr_6O_4(OH)_4$(BDC-NH_2)$_6$ in the framework of UiO-66-NH_2, probably originated from some missing-linker defects.[44] Fortunately, the UiO-66-NH_2 structure possesses good resistance to linker vacancies without the crystal structure collapse due to the high coordination numbers of Zr clusters. The good tolerance to linker vacancies also means that the organic struts in their frameworks could be exchangeable.[37] Besides, the missing-linker defects in UiO-66-NH_2 would make the OH^- complete the Zr-coordination sphere and form missing-linker-induced Zr-OH groups.[45] These resultant exposed Zr-OH groups provide more binding sites as recognition centers toward P-O bonds of phosphate, which is favourable for the highly selective detection of phosphate in aqueous solution.

Optical spectra properties of UiO-66-NH_2

To get the knowledge about the interaction between the Zr-O nodes and organic struts of BDC-NH_2 in the synthesized MOFs, the DR-UV-Vis spectra (**Fig. S4, ESI†**) of UiO-66-NH_2 and BDC-NH_2 ligands were investigated at room temperature. It is found that free BDC-NH_2 ligands exhibit an intense absorption band from 290 to 500 nm with an absorption peak at 381 nm, presumably attributed to $\pi \rightarrow \pi^*$ electronic transition of aromatic ring.[46] A blue-shift to 368 nm is observed in the absorption peak of UiO-66-NH_2 powder as compared to the free ligand, which is attentively assigned to the ligand-to-metal charge transfer (LMCT).[41,47] Obviously, this LMCT effect could be greatly mediated by the coordination status of Zr-O clusters in UiO-66-NH_2.

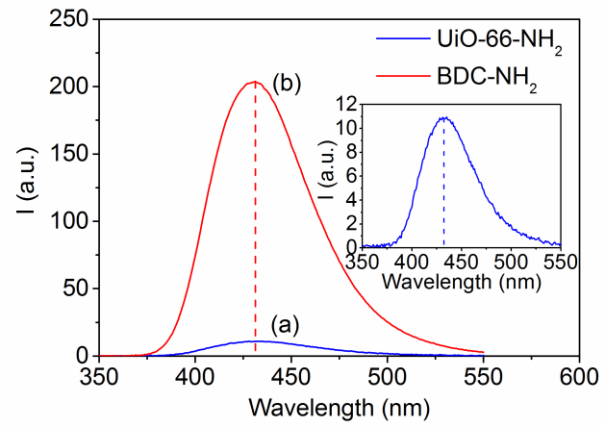

Fig. 2 Fluorescence emission spectra of the (a) free BDC-NH_2 ligand and (b) UiO-66-NH_2 (50 mg L^{-1} for each) in HEPES buffer solution (pH = 7, 20 mmol) under excitation at 328 nm. The inset presents the enlarged profile of fluorescent emission from UiO-66-NH_2 MOFs.

Interestingly, UiO-66-NH_2 in aqueous solution exhibits a weak fluorescence emission peak at 431 nm, which is approximate twenty times lower than that of the free BDC-NH_2 ligands (**Fig. 2**). Except the above LMCT effect, we cannot rule out that the solvent-induced fluorescence quenching effect also plays an important role in weakening the fluorescence of UiO-66-NH_2 suspension, which is largely dependent on the polarity of solvent molecules and their coupling with Zr-O nodes as reported.[48] When the guest molecules of H_2O enter the cavities, they interact with Zr-O clusters *via* weak hydrogen bond and may affect the electron transfer between Zr-coordination sphere and BDC-NH_2.[49] It is also found that the weak emission from UiO-66-NH_2 MOFs (**Fig. S5, ESI†**) is very stable in aqueous solution as verified by a day-to-day fluorescence measurement, resulting from their good chemical stability. This endows them with the feasibility as a fluorescent probe in aqueous solution.

Kinetics for the fluorescence sensing of phosphate

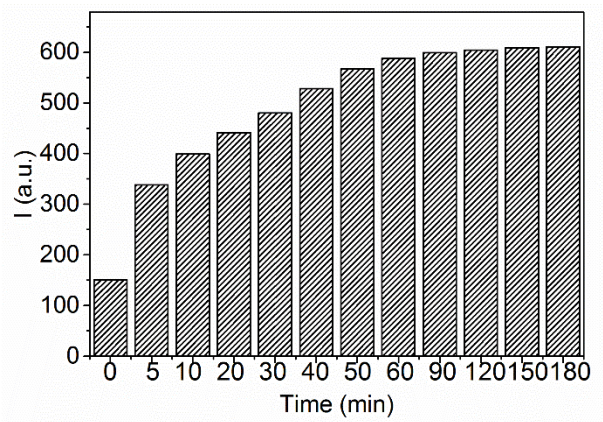

Fig. 3 Effect of incubation time on the fluorescent intensity upon the addition of the phosphate into the UiO-66-NH_2 MOFs detection system (phosphate concentration was set as 100 μM).

To understand the effect of host-guest contact time on the fluorescence sensing of phosphate, the kinetics for the sensing were measured with the phosphate concentration of 100 μM in HEPES buffer solution (pH = 7). As shown in **Fig. 3**, the emission from UiO-66-NH_2 suspension increases quickly in the first 5 min and gradually reaches the fluorescence equilibrium at approximate 90 min. In the initial period, abundant recognition sites of Zr-O clusters in UiO-66-NH_2 are available, leading to the quick phosphate coordination to the binding sites and the corresponding rapid fluorescence enhancement. Additionally, small molecular size of phosphate could facilitate its diffusion into the cavities of UiO-66-NH_2 probes, probably also having a positive effect on the fluorescence response rate. After that, the decreased amount of available recognition sites gives rise to the lower phosphate complexation rate, resulting in the subsequent slow and final saturated fluorescent intensity. Therefore, a 90 min incubation time was selected for the following sensing property investigation to ensure reaching the fluorescence equilibrium for the phosphate assay.

Selective sensing phosphate with UiO-66-NH_2 fluorescent probe

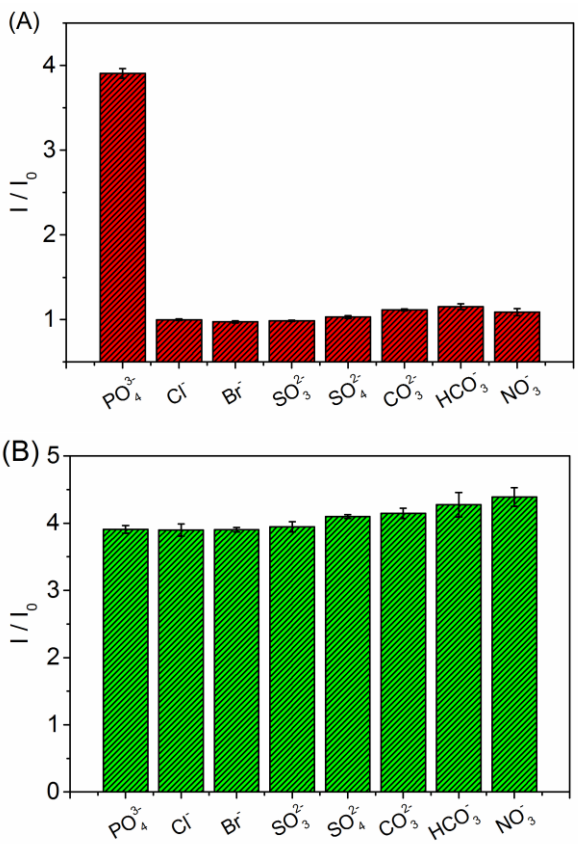

Fig. 4 (A) The fluorescence response of UiO-66-NH_2 (50 mg L^{-1}) in HEPES (pH = 7, 20 mmol) towards various anions (100 μM for each). (B) Effects of coexistent anions (100 μM for each) on the fluorescence response of UiO-66-NH_2 in HEPES with the addition of 100 μM phosphate. I_0 and I denote the fluorescence intensity of UiO-66-NH_2 in HEPES without and with anions, respectively (λ_{ex} = 328 nm, λ_{em} = 431 nm).

To check the potentials of UiO-66-NH_2 as fluorogenic sensor for the phosphate detection, the fluorescence response of UiO-66-NH_2 suspension in the presence of various anions, including Cl^-, Br^-, SO_4^{2-}, SO_3^{2-}, CO_3^{2-}, HCO_3^-, NO_3^-, was recorded in HEPES

buffer solution (pH = 7). **Fig. 4A** illustrates the fluorescence variations upon the addition of 100 μM various anions to UiO-66-NH_2 suspension (50 mg L^{-1}). As expected, no obvious fluorescence changes are observed for the other anions while the fluorescence intensity proceeds 4 times enhancement upon the addition of phosphate to the suspension, evidencing the special recognition capability of UiO-66-NH_2 to phosphate in aqueous solution.

Since the high specificity is crucial for most probes to be applied in the real sample detection, we further added other anions to the UiO-66-NH_2-phosphate detection system. No significant fluorescence changes occur in the experiments in which other anions were spontaneously added into the phosphate-containing detecting systems (**Fig. 4B**). These findings confirm that the current UiO-66-NH_2 fluorescent probe is effective for the selective phosphate detection with good anti-interference ability to co-existent anions. As a control experiment, the capability of free BDC-NH_2 ligand to detect various anions was also checked (**Fig. S6, ESI†**). No obvious fluorescence responses are observed upon the addition of phosphate or other anions to BDC-NH_2 solution, further indicating that the coordination of Zr-O clusters to BDC-NH_2 ligands in the framework of UiO-66-NH_2 plays key roles in the selective detection of phosphate.

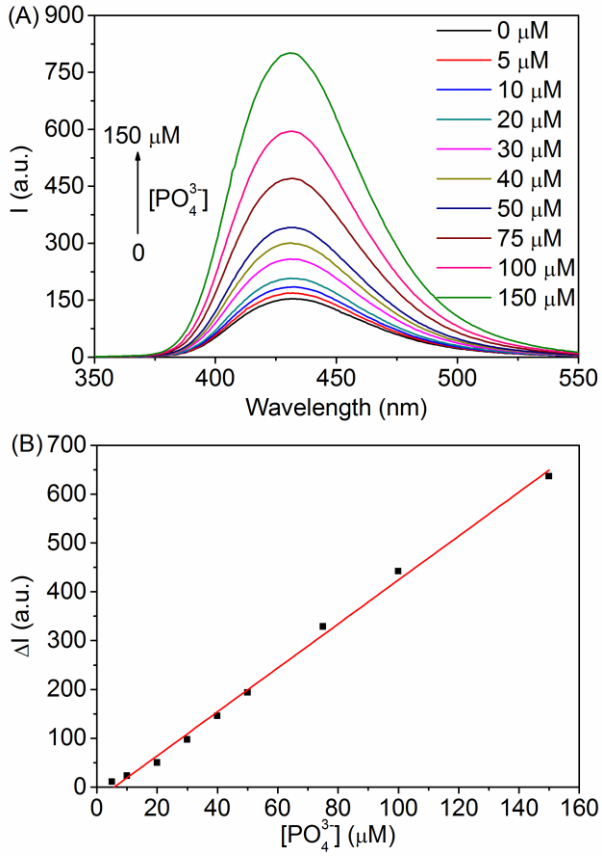

Fig. 5 (A) The evolvement of the fluorescence spectra of UiO-66-NH_2 (50 mg L^{-1}) suspension in HEPES (pH = 7, 20 mmol) upon the addition of various concentrations of phosphate under excitation at 328 nm. (B) Linear plots of the enhanced fluorescence intensity from UiO-66-NH_2 suspension as a function of phosphate concentration. ΔI is the enhanced intensity from UiO-66-NH_2 suspension in the absence and presence of phosphate.

To test the sensitivity of UiO-66-NH_2 for the phosphate detection, fluorescence titration spectra with different phosphate concentration were conducted with an excitation wavelength at 328 nm at room temperature. Upon gradual addition of phosphate anions (from 0 to 150 μM) to the UiO-66-NH_2 suspension, the fluorescence intensity is gradually increased (**Fig. 5A**). When the phosphate is added up to 150 μM, about five-fold fluorescent enhancement is observed. Furthermore, the fluorescence sensing of UiO-66-NH_2 has a good linear correlation (R^2 = 0.996) in the range of 5-150 μM phosphate (**Fig. 5B**). The detection limit is estimated to be 1.25 μM (3σ/sensitivity), which is far below the detection requirement of phosphate discharge criteria in the water environment, reported to be around 0.2-10 mg P/L (6.4-320 μM).[1]

Possible sensing mechanism for phosphate detection

To get in-depth understand the possible mechanism of the current fluorescent probe for the phosphate detection, FT-IR and XPS were conducted to exploit the interaction between phosphate and the framework of UiO-66-NH_2. For pristine UiO-66-NH_2 (**Fig. 6b**), the absorption peaks between 600-800 cm^{-1} correspond to Zr-O_2 as longitudinal and transverse modes. The intense doublet at 1415 and 1387 cm^{-1} (labelled with red stars) can be assigned to the stretching modes of the carboxylic groups in BDC-NH_2 ligands.[50] After the incubation with phosphate aqueous solution, the broad P-O stretching vibration bands between 900 and 1200 cm^{-1} appear, confirming the inclusion of phosphate molecules into UiO-66-NH_2.[51] Furthermore, an obvious red shift of IR absorption from 1100 to 1028 cm^{-1} occurs for the P-O bonds in the UiO-66-NH_2(P) as compared to the free phosphate (**Fig. 6**). This might imply the occurrence of complexation between phosphoric groups and Zr-O clusters since the tether of P-O bonds could limit their stretching vibration and consequently decrease their vibration frequency. On the contrary, the symmetric stretching vibrations of carboxylic groups in UiO-66-NH_2(P) demonstrate a blue shift to 1430 and 1393 cm^{-1}. This might give further evidence that phosphate has a coordination effect with Zr-O clusters and weakens the interaction between the BDC-NH_2 ligands and Zr clusters, thus making the carboxylic groups more free and their vibration stronger.[35]

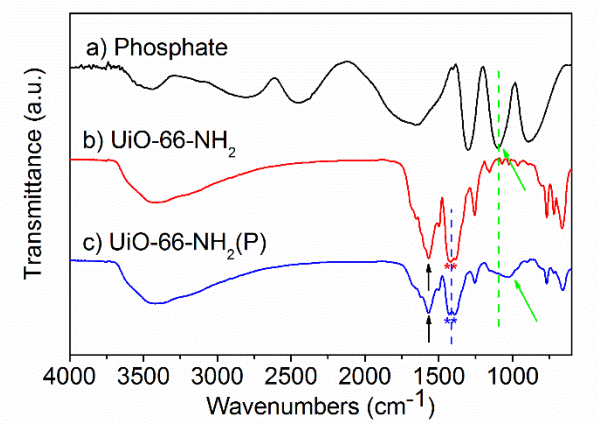

Fig. 6 FT-IR spectra of the (a) free phosphate, (b) UiO-66-NH_2 and (c) UiO-66-NH_2(P). UiO-66-NH_2(P) was the collected powder after the incubation of UiO-66-NH_2 with phosphate (P : Zr molar ratio was 0.6:1 in the solution) for 90 min.

We also measured XPS spectra of P, O and Zr of UiO-66-NH_2(P) to further provide the information of the host-guest interaction. The appearance of P2p peak verifies that the phosphate is undoubtedly attracted into UiO-66-NH_2 (**Fig. S7, ESI†**) in agreement with FT-IR analysis. The deconvoluted O1s spectrum in UiO-66-NH_2(P) (**Fig. S8, ESI†**) consists of four peaks, which might be ascribed to O in O-C=O (533.7 eV), P-O-H (532.6 eV), Zr-O-Zr (530.0 eV), and in Zr-O-P and P=O (531.5 eV).[36,52] Although the differences of O1s XPS spectra between parent UiO-66-NH_2 and UiO-66-NH_2(P) (**Fig. S8, ESI†**) seemingly evidences the evolvement of P-O-Zr bond, it is difficult to differentiate the O signals from the organic ligands, $Zr_6O_4(OH)_4$ clusters or phosphate. In Zr3d spectra, two peaks at 182.56 and 184.88 eV could be attributed to Zr-O clusters coordinated with the carboxylic groups of BDC-NH_2 ligands in UiO-66-NH_2 (**Fig. 7a**).[53] These peaks shift to 182.78 and 185.18 eV for UiO-66-NH_2(P) (**Fig. 7b**). The shift of binding energy to higher might be due to the replacement of carboxylic groups coordinated with Zr-O clusters by phosphoric groups. Bonding to more electro-negative P-O bonds leads to the loss of electron density at zirconium, which in turn raises its 3d electrons binding energies.[54] This would partially interrupt the electron transfer between organic ligands of BDC-NH_2 and inorganic nodes of Zr-O clusters in UiO-66-NH_2 and consequently recover the fluorescence of BDC-NH_2 in perfectly coincident with our proposed sensing mechanism.

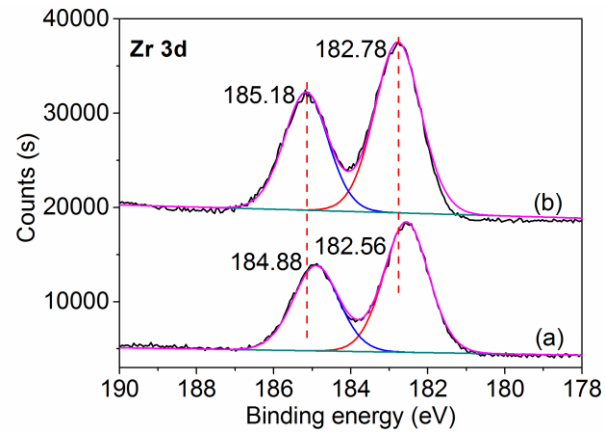

Fig. 7 XPS spectra of Zr3d electrons for UiO-66-NH_2 (a) and UiO-66-NH_2(P) (b). UiO-66-NH_2(P) was the collected powder samples after the incubation of UiO-66-NH_2 with phosphate solution (P : Zr molar ratio was set as 0.6:1 in the solution) for 90 min.

To explore the structure-property correlation, the structure change of UiO-66-NH_2 framework incubated with progressively increased phosphate was also monitored by XRD, BET and TEM. At the low range of P : Zr molar ratio (0~0.3) in solution, almost no obvious change could be observed in XRD patterns (**Fig. 8**). The phosphate might firstly occupy the missing-linker defects or substitute trace amount of carboxylic groups in BDC-NH_2 ligands, so that the structure of UiO-66-NH_2 are stably maintained benefiting from the high coordination numbers of Zr-O clusters in the ZrMOFs. With the gradual increasing of phosphate level to P : Zr molar ratio of high up to 0.6 : 1, more and more phosphate coordinates with the Zr-O clusters, which might make the bicipital BDC-NH_2 suspend in the framework, leading to a slight change of structure integrity (**Fig. 8i**). At this point, the TEM image (**Fig. S2B, ESI†**) shows that the UiO-66-NH_2(P) still keeps the crystalline morphology, indicating that the partial replacement of the BDC-NH_2 ligand by monofunctional phosphate would lead to a slight decrease of structure integrity, but the morphology is not destroyed. The surface area of UiO-66-NH_2(P) also reduces to 460 from 671 m^2/g of pristine UiO-66-NH_2 (**Fig. S9, ESI†**). The above results demonstrate that the structure of fluorescent UiO-66-NH_2 MOFs is closely related to the addition of phosphate due to its competitive coordination effect. The interaction between the carboxylic groups of BDC-NH_2 ligands and Zr-O clusters gradually weakens upon the consecutive addition of phosphate, and the fluorescence of BDC-NH_2 proportionally recovered in correction with the applied level of phosphate for detection.

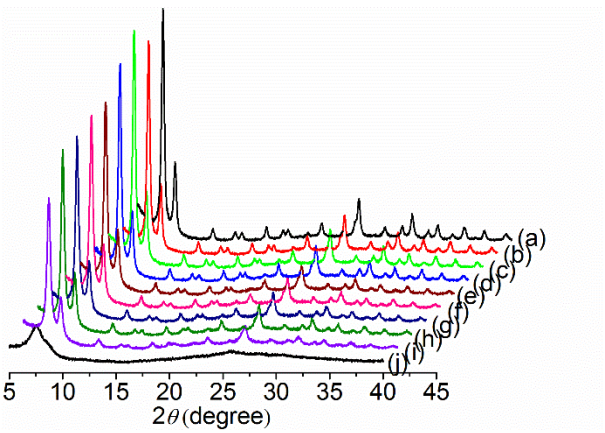

Fig. 8 Powder XRD patterns of UiO-66-NH_2 MOFs after their contacting with the phosphate solution at P : Zr molar ratios of 0 (a), 0.006 (b), 0.03 (c) 0.06 (d), 0.12 (e), 0.18 (f), 0.24 (g), 0.3 (h), 0.6 (i) and 3 (j).

Conclusions

In summary, a simple fluorescent sensor based on Zr-based MOF has been successfully developed for the selective and sensitive assay of the anionic phosphate in aqueous solution. The inorganic Zr-O clusters and organic BDC-NH_2 linkers in the elaborated UiO-66-NH_2 MOFs are individually designed as phosphate recognition sites and signal reporters. The specific coordination of phosphate with Zr-O clusters weakens the interaction between inorganic nodes and organic struts and proportionally recovers the intrinsic fluorescence of BDC-NH_2 ligands in correlation with the applied phosphate level. This strategy paves a new way to design selective MOF-based sensors for detection of other analytes based on different functions of organic and inorganic components in MOFs. Given the fact that Zr-based MOFs possess high chemical stability and could be scaled up to produce with various organic units, this would expand their applications in the fields of chemical and biological sensing.

Acknowledgment

This work was financially supported by the Natural Science

Foundation of China (51072053, 51372084), the Innovation Program of Shanghai Municipal Education Commission (13zz040), the Nano-Special Foundation for Shanghai Committee of Science and Technology (12nm0502600) and the 111 Project (B14018).

Notes and references

*Key Laboratory for Ultrafine Materials of Ministry of Education, School of Materials Science and Engineering, East China University of Science and Technology, Shanghai 200237, China. Fax: +86-21-64250740; Tel: +86-21-64252599; E-mail: **jinlougu@ecust.edu.cn***

† Electronic Supplementary Information (ESI) available: N_2 sorption isotherms, TEM images, DR-UV-Vis spectra and wide scan, O1s XPS spectra of parent UiO-66-NH_2 and UiO-66-NH_2(P), TG-DTA profile, fluorescence spectra for UiO-66-NH_2 and fluorescence response curves of BDC-NH_2 to different anionic ions. See DOI: 10.1039/b000000x/

1 W. Cheng, J. Sue, W. Chen, J. Chang and J. Zen, *Anal. Chem.*, 2009, **82**, 1157.
2 K. Wygladacz, Y. Qin, W. Wroblewski and E. Bakker, *Anal. Chim. Acta*, 2008, **614**, 77.
3 W. C. Mak, C. Chan, J. Barford and R. Renneberg, *Biosens. Bioelectron.*, 2003, **19**, 233.
4 S. Cosnier, C. Gondran, J. Watelet, W. De Giovani, R. P. M. Furriel and F. A. Leone, *Anal. Chem.*, 1998, **70**, 3952.
5 H. Sun, A. M. Scharff-Poulsen, H. Gu, I. Jakobsen, J. M. Kossmann, W. B. Frommer and K. Almdal, *ACS Nano*, 2008, **2**, 19.
6 M. A. Rahman, D. Park, S. Chang, C. J. McNeil and Y. Shim, *Biosens. Bioelectron.*, 2006, **21**, 1116.
7 H. X. Zhao, L. Q. Liu, Z. D. Liu, Y. Wang, X. J. Zhao and C. Z. Huang, *Chem. Commun.*, 2011, **47**, 2604.
8 Z. Yang, M. Wang, A. M. Yong, S. Y. Wong, X. Zhang, H. Tan, A. Y. Chang, X. Li and J. Wang, *Chem. Commun.*, 2011, **47**, 11615.
9 P. D. Beer and P. A. Gale, *Angew. Chem. Int. Ed.*, 2001, **40**, 486.
10 S. Khatua, S. H. Choi, J. Lee, K. Kim, Y. Do and D. G. Churchill, *Inorg. Chem.*, 2009, **48**, 2993.
11 O. M. Yaghi, M. O'Keeffe, N. W. Ockwig, H. K. Chae, M. Eddaoudi and J. Kim, *Nature*, 2003, **423**, 705.
12 S. Kitagawa, R. Kitaura and S. Noro, *Angew. Chem. Int. Ed.*, 2004, **43**, 2334.
13 G. Férey, *Chem. Soc. Rev.*, 2008, **37**, 191.
14 B. Chen, S. Xiang and G. Qian, *Acc. Chem. Res.*, 2010, **43**, 1115.
15 L. E. Kreno, K. Leong, O. K. Farha, M. Allendorf, R. P. Van Duyne and J. T. Hupp, *Chem. Rev.*, 2011, **112**, 1105.
16 Z. Hu, B. J. Deibert and J. Li, *Chem. Soc. Rev.*, 2014, **43**, 5815.
17 D. Liu, K. Lu, C. Poon and W. Lin, *Inorg. Chem.*, 2014, **53**, 1916.
18 Z. Dou, J. Yu, Y. Cui, Y. Yang, Z. Wang, D. Yang and G. Qian, *J. Am. Chem. Soc.*, 2014, **136**, 5527.
19 Y. Cui, Y. Yue, G. Qian and B. Chen, *Chem. Rev.*, 2012, **112**, 1126.
20 Z. Xiang, C. Fang, S. Leng, D. Cao, *J. Mater. Chem. A*, 2014, **2**, 7662.
21 G. Y. Wang, C. Song, D. M. Kong, W. J. Ruan, Z. Chang and Y. Li, *J. Mater. Chem. A*, 2014, **2**, 2213.
22 L. Dobrzańska, G. O. Lloyd, C. Esterhuysen and L. J. Barbour, *Angew. Chem. Int. Ed.*, 2006, **45**, 5856.
23 S. M. Barrett, C. Wang and W. Lin, *J. Mater. Chem.*, 2012, **22**, 10329.
24 C. Yang, H. Ren and X. Yan, *Anal. Chem.*, 2013, **85**, 7441.
25 K. L. Wong, G. L. Law, Y. Y. Yang and W. T. Wong, *Adv. Mater.*, 2006, **18**, 1051.
26 B. Chen, L. Wang, F. Zapata, G. Qian and E. B. Lobkovsky, *J. Am. Chem. Soc.*, 2008, **130**, 6718.
27 A. Lan, K. Li, H. Wu, D. H. Olson, T. J. Emge, W. Ki, M. Hong and J. Li, *Angew. Chem. Int. Ed.*, 2009, **48**, 2334.
28 Y. Xiao, Y. Cui, Q. Zheng, S. Xiang, G. Qian and B. Chen, *Chem. Commun.*, 2010, **46**, 5503.
29 H. L. Jiang, D. Feng, K. Wang, Z. Y. Gu, Z. Wei, Y. P. Chen and H. C. Zhou, *J. Am. Chem. Soc.*, 2013, **135**, 13934.
30 J. N. Hao and B. Yan, *J. Mater. Chem. A*, 2014, **2**, 18018.
31 Y. Zhou, H. H. Chen and B. Yan, *J. Mater. Chem. A*, 2014, **2**, 13691.
32 D. Tian, Y. Li, R. Y. Chen, Z. Chang, G. Y. Wang and X. H. Bu, *J. Mater. Chem. A*, 2014, **2**, 1465.
33 Y. S. Xue, Y. He, L. Zhou, F. J. Chen, Y. Xu, H. B. Du, X. Z. You and B. Chen, *J. Mater. Chem. A*, 2013, **1**, 4525.
34 D. Zhao, X. Wan, H. Song, L. Hao, Y. Su and Y. Lv, *Sens. Actuators B*, 2014, **197**, 50.
35 X. Zhu, J. Gu, Y. Wang, B. Li, Y. Li, W. Zhao and J. Shi, *Chem. Commun.*, 2014, **50**, 8779.
36 X. Zhu, B. Li, J. Yang, Y. Li, W. Zhao, J. Shi, J. Gu, *ACS Appl. Mater. Interfaces*, 2015, **7**, 223.
37 J. H. Cavka, S. Jakobsen, U. Olsbye, N. Guillou, C. Lamberti, S. Bordiga and K. P. Lillerud, *J. Am. Chem. Soc.*, 2008, **130**, 13850.
38 A. Schaate, P. Roy, A. Godt, J. Lippke, F. Waltz, M. Wiebcke and P. Behrens, *Chem. Eur. J.*, 2011, **17**, 6643.
39 H. Wu, Y. S. Chua, V. Krungleviciute, M. Tyagi, P. Chen, T. Yildirim and W. Zhou, *J. Am. Chem. Soc.*, 2013, **135**, 10525.
40 B. J. Deibert and J. Li, *Chem. Commun.*, 2014, **50**, 9636-9639.
41 L. Shen, R. Liang, M. Luo, F. Jing and L. Wu, *Phys. Chem. Chem. Phys.*, 2015, **17**, 117.
42 M. J. Katz, Z. J. Brown, Y. J. Colon, P. W. Siu, K. A. Scheidt, R. Q. Snurr, J. T. Hupp and O. K. Farha, *Chem. Commun.*, 2013, **49**, 9449.
43 J. Gu, W. Fan, A. Shimojima and T. Okubo, *Small*, 2007, **3**, 1740.
44 F. Vermoortele, B. Bueken, G. Le Bars, B. Van de Voorde, M. Vandichel, K. Houthoofd, A. Vimont, M. Daturi, M. Waroquier, V. Van Speybroeck, C. Kirschhock and D. E. De Vos, *J. Am. Chem. Soc.*, 2013, **135**, 11465.
45 H. G. T. Nguyen, N. M. Schweitzer, C.-Y Chang, T. L. Drake, M. C. So, P. C. Stair, O. K. Farha, J. T. Hupp and S. T. Nguyen, *ACS Catalysis*, 2014, **4**, 2496.
46 J. He, J. Wang, Y. Chen, J. Zhang, D. Duan, Y. Wang and Z. Yan, *Chem. Commun.*, 2014, **50**, 7063.
47 C. G. Silva, I. Luz, F. X. Llabrés I Xamena, A. Corma and H. Garcá, *Chem. Eur. J.*, 2010, **16**, 11133.
48 W. Zhang, H. Huang, D. Liu, Q. Yang, Y. Xiao, Q. Ma and C. Zhong, *Micropor. Mesopor. Mater.*, 2013, **171**, 118.
49 Z.-Z. Lu, R. Zhang, Y.-Z. Li, Z.-J Guo and H.-G Zheng, *J. Am. Chem. Soc.*, 2011, **133**, 4172.
50 L. Valenzano, B. Civalleri, S. Chavan, S. Bordiga, M. H. Nilsen, S. Jakobsen, K. P. Lillerud and C. Lamberti, *Chem. Mater.*, 2011, **23**, 1700-1718.
51 C. Luengo, M. Brigante, J. Antelo and M. Avena, *J. Colloid Interf. Sci.*, 2006, **300**, 511.
52 K. C.-W. Wu, Y. Yamauchi, C.-Y Hong, Y.-H Yang, Y.-H Liang, T. Funatsu and M. Tsunoda, *Chem. Commun.*, 2011, **47**, 5232.
53 Q. Wu, D. Wu and Y. Guan, *Anal. Chem.*, 2014, **86**, 10122-10130.
54 Y. M. Zheng, L. Yu and J. P. Chen, *J. Colloid Interf. Sci.*, 2012, **367**, 362.

Metal-organic frameworks with inherent recognition sites for selective phosphate sensing through their coordination-induced fluorescence enhancement effect

Jian Yang, Yan Dai, Xiangyang Zhu, Zhe Wang, Yongsheng Li, Qixin Zhuang, Jianlin Shi, and Jinlou Gu*

Zr-O clusters and BDC-NH_2 linkers in Zr-MOFs are individually designed as recognition sites and fluorescent reporters for phosphate sensing.